18th International Conference on Information Fusion
Washington, DC - July 6-9, 2015

MMOSPA-based Direction-of-Arrival Tracking with a Passive Sonar Array – An Experimental Study

Marcus Baum and **Peter Willett**
University of Connecticut, CT, USA.
Email: baum@engineer.uconn.edu, willett@engr.uconn.edu

***Abstract*—We consider the directions-of-arrival tracking of multiple narrowband waveforms impinging on a sonar array. As the captured measurements do not provide any information about the labeling of the objects, a challenge is to resolve the directions-of-arrival coming from closely-spaced objects. In order to prevent track coalescence, we pursue the recently introduced concept of Minimum Mean OSPA (MMOSPA) estimation and propose a Gaussian particle filter that is tailored to the Optimal Sub-Pattern Assignment (OSPA) distance for sets. The main contribution of this work is to illustrate the benefits of MMOSPA estimation with a real data set from a large-aperture passive sonar array mounted in the east of Ft. Lauderdale in Florida, USA.**

I. Introduction

A sensor array such as a sonar or a radar array [17], [24], [25], [28], [31] consists of several individual sensors arranged in a specific geometric pattern. In this manner, a sensor array allows for an increased directional gain and a quick adjustment of the scan direction. A fundamental signal processing task for sensor arrays is the determination of the directions-of-arrival (DOAs) of impinging signals. As measurements from narrowband signals captured with a sensor array do not provide any information about the labeling of the objects, a major challenge is to separate directions-of-arrival of closely-spaced objects. Traditional methods are MUSIC [31], which is based on a spectral decomposition, and both Maximum Likelihood (ML) and Maximum a Posteriori (MAP) estimators [28].

Recent works [3], [10], [11] discussed coalescence effects of ML/MAP and Minimum Mean Squared Error (MMSE) estimates for DOAs in the case of extremely closely-spaced objects. The reason is that the likelihood function is symmetric with respect to objects labels, i.e., it is impossible to find out which object is which. A solution is to ignore the object labels inherently by means of using the concept of Minimum Mean OSPA (MMOSPA) estimation [3], [9]–[11], [18], [29]. As a MMOSPA estimator is based on the Optimal Sub-Pattern Assignment (OSPA) metric [27] for sets, it allows for a well-grounded incorporation of symmetric likelihood functions. Several multi-target tracking algorithms that are optimized with respect to the OSPA distance have been developed, e.g., there is the Set-JPDAF [29], the Set Multiple Hypothesis Tracker (MHT) [13], and tailored particle filters [16]. Much of the groundwork for random finite set (RFS) estimation and filtering was laid by Mahler, see for example [22], [23].

In this work, we demonstrate the benefits of MMOSPA techniques for directions-of-arrival tracking by means of a real data set captured as part of “The Shallow Water Array Performance (SWAP)” project [7], [19], [26]. For this purpose, we develop a MMOSPA-tailored Gaussian particle filter (named in the following Set-GPF) that is capable of tracking directions-of-arrival over time without suffering from coalescence. The experiments clearly show that the Set-GPF is capable of tracking two closely-spaced objects while the standard Gaussian particle filter suffers from significant track coalescence.

The SWAP data set has also been used in [21] for evaluating a fuse-before-track approach for multi-object tracking. While [21] focuses on the fusion of Bearing-Time Records (BTRs) from different sub-arrays, our approach directly works with the captured raw data as our focus is to resolve closely-spaced objects as good as possible. There are several works about particle filtering techniques for DOA estimation, e.g., [30], [33], [34]. The objective of this paper is not to compare different particle filters for DOA estimation; we want to demonstrate the benefits of MMOSPA estimation by comparing a particle filter with and without MMOSPA enhancement.

II. Problem Description

We consider a large-aperture passive sonar array in a shallow-water environment, which is investigated as part of the “The Shallow Water Array Performance (SWAP)” project [7], [19], [26]. The array is located in the east of Ft. Lauderdale in Florida. It consists of 475 hydrophones and is approximately 900 meters long. We are interested in tracking the directions-of-arrival of waveforms impinging on the sonar array. As a ground truth, the Automatic Identification System (AIS) data from surface ships in the surveillance region is available. A map of the setting is shown in Fig. 1a and the Bearing-Time Record (BTR) for the considered time span is depicted in Fig. 1b. The BTR, which is the standard method to display sonar data, plots the received energy from all directions over time.

For our experimental analysis, we assume that the number of objects N_t in the surveillance region is known. For each object/ship, we aim at tracking the direction-of-arrival of the impinging wavefront. We consider a scenario where ships cannot be differentiated via their acoustic signatures. All signals are assumed to be narrowband with known carrier frequency but unknown complex amplitude. The direction-of-arrival of a sound source is modeled to evolve over time according to a discrete-time constant velocity model. Hence, the state vector $\underline{x}_k^l$ of the l-th object, $l = 1, \ldots, N_t$, at discrete time k is given by

$$\underline{x}_k^l = \left[\theta_k^l, \dot{\theta}_k^l\right]^T \quad , \tag{1}$$

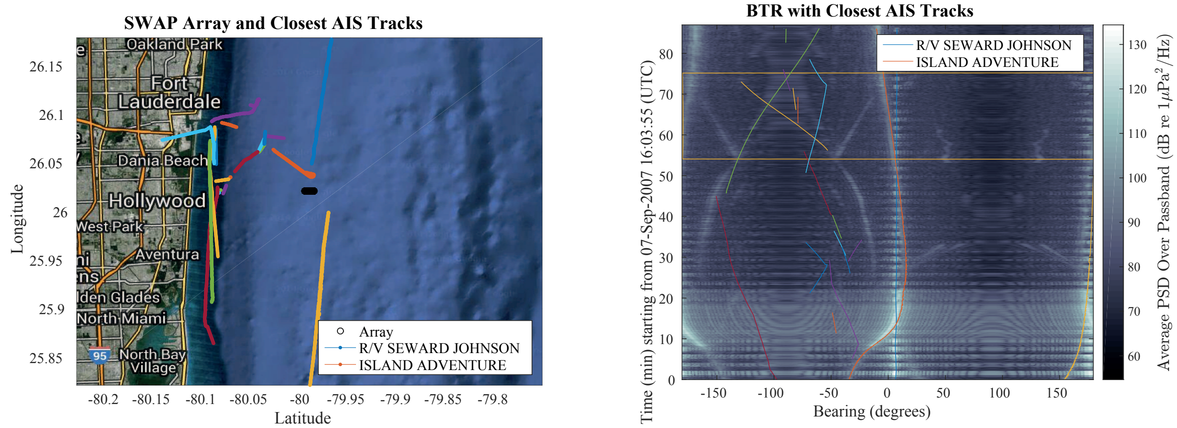

(a) Map of the surveillance region including the sonar array and the AIS tracks of the closest ships.

(b) Bearing-Time Record (BTR) and closest ships (according to AIS information).

Fig. 1: Setting of the SWAP experiment in the east of Ft. Lauderdale, Florida, on September 7, 2007.

where θ_k^l denotes the direction-of-arrival and $\dot{\theta}_k^l$ is the DOA rate. The system equation for the constant velocity model is

$$\underline{x}_k^l = \mathbf{A} \cdot \underline{x}_{k-1}^l + \underline{w}_k^l \ , \tag{2}$$

where

- $\mathbf{A}^l = \begin{pmatrix} 1 & \Delta T \\ 0 & 1 \end{pmatrix}$ is the system matrix with scan period ΔT and
- $\underline{w}_k^l$ is white Gaussian system noise with covariance matrix $\mathbf{C}_w = q_0 \begin{pmatrix} \frac{\Delta T^4}{4} & \frac{\Delta T^2}{2} \\ \frac{\Delta T^2}{2} & \Delta T^2 \end{pmatrix}$ and parameter q_0.

As the ships might be close together (in DOA space), we aim at estimating the joint state vector of all ships, i.e.,

$$\underline{x}_k := \left[(\underline{x}_k^1)^T, \ldots, (\underline{x}_k^{N_t})^T\right]^T \in \mathbb{R}^{2 \cdot N_t} \tag{3}$$

where, as implied in our MMOSPA discussion, the ordering amongst the N_t contacts in (3) is immaterial. Finally, we obtain the joint system equation

$$\underline{x}_{k+1} = \mathbf{A}\underline{x}_k + \underline{w}_k \tag{4}$$

with $\mathbf{A} = \mathrm{diag}(\mathbf{A}^1, \ldots, \mathbf{A}^{N_t})$ and $\underline{w}_k = \left[(\underline{w}_k^1)^T, \ldots, (\underline{w}_k^{N_t})^T\right]^T$.

A. Signal Processing

The raw data from the hydrophones is acquired with sampling frequency 1 kHz. As described in [19], we apply a short-term Fourier transform to each hydrophone time series in order to transfer to the frequency domain (1024 bins, 50% overlap). In this manner, a complex spectrum output is obtained every 0.5 s.

B. Measurement Model

The sonar array consists of N_a hydrophones with known locations $\underline{c}^1, \ldots, \underline{c}^{N_a} \in \mathbb{R}^2$ in two-dimensional space, where we assume that the first hydrophone is located at the origin, i.e., $\underline{c}^1 = [0, 0]^T$.

Each sound source (i.e., ship) emits a planar wavefront impinging on the sonar array. The time difference of the planar wavefront from the l-th ship with respect to the first hydrophone $\underline{c}^1$ is given by

$$d^{l,m}(\underline{x}_k^l) = (\underline{c}^m)^T \underline{r}_k^l \ ,$$

where $\underline{r}_k^l = \left[\cos(\theta_k^l), \sin(\theta_k^l)\right]^T$.

For narrowband signals, time-delays result in phase shifts so that the complex envelope of the received signal z_k^m at the m-th hydrophone becomes [3], [17], [24], [25], [28], [31]

$$z_k^m = \sum_{l=1}^{N_t} h^m(\underline{x}_k^l) \cdot s_k^l + v_k^m \ , \tag{5}$$

where

- s_k^l is the unknown complex signal of l-th ship, which is distributed according to a zero-mean complex Gaussian random variable,
- $h^m(\underline{x}_k^l) = e^{j \frac{2\pi}{\lambda} d^{l,m}(\underline{x}_k^l)}$ denotes the response of the m-th hydrophone to a signal with wavelength λ, and
- v_k^m models additive zero-mean Gaussian noise.

By defining the stacked measurement vector $\underline{z}_k = \left[z_k^1, \ldots, z_k^{N_a}\right]^T \in \mathbb{R}^{N_a}$, the overall measurement equation becomes

$$\underline{z}_k = \mathbf{H}(\underline{x}_k) \cdot \underline{s}_k + \underline{v}_k \tag{6}$$

with array response matrix $\mathbf{H}(\underline{x}_k) = (h^m(\underline{x}_k^l))_{m,l} \in \mathbb{R}^{N_a \cdot N_t}$ and stacked noise vector $\underline{v}_k = \left[v_k^1, \ldots, v_k^{N_a}\right]^T \in \mathbb{R}^{N_a}$. From (6), the following likelihood function can be derived

$$p(\underline{z}_k \,|\, \underline{x}_k) = \mathcal{CN}(\underline{z}_k - \underline{0}, \mathbf{C}_v + \mathbf{H}(\underline{x}_k)\mathbf{C}_s(\mathbf{H}(\underline{x}_k))^H) \ , \tag{7}$$

which is a zero-mean complex Gaussian distribution with a covariance matrix that depends on the covariance matrix $\mathbf{C}_s$ of the signals $\underline{s}_k^l$ and the covariance matrix $\mathbf{C}_v$ of the noise $\underline{v}_k$.

III. Gaussian Particle Filter for DOA Estimation

The purpose of this paper is to demonstrate the effectiveness of MMOSPA estimation and tracking on real data. To this end, we discuss an extant multi-target tracking algorithm, the Gaussian Particle Filter. The GPF *may* be used directly. However, in the following we discuss its shortcomings – in terms of track coalescence – and in the following section we re-work it with MMOSPA in mind. By using a fixed algorithm, respectively without and with our MMOSPA enhancement, it is hoped that the benefits be clear. We make no special claim that the GPF is the best tracker; that is not our point.

Based on the system and measurement model introduced in Section II, the objective is to recursively calculate the posterior density of the joint state vector (3)

$$p(\underline{x}_k|Z_k) \ , \tag{8}$$

where $Z_k := \{\underline{z}_1, \ldots, \underline{z}_k\}$. For this purpose, alternating prediction and measurement update steps are performed, where the prediction step is given by

$$p(\underline{x}_k|Z_{k-1}) = \int p(\underline{x}_k|\underline{x}_{k-1}) \cdot p(\underline{x}_{k-1}|Z_{k-1}) \ d\underline{x}_{k-1} \tag{9}$$

and the measurement update step follows from Bayes rule

$$p(\underline{x}_k|Z_k) = c \cdot p(\underline{z}_k|\underline{x}_k) \cdot p(\underline{x}_k|Z_{k-1}) \tag{10}$$

with normalization constant c.

In this work, we aim at a Gaussian state estimator, i.e., the posterior density (10) and prediction (9) are approximated as Gaussians according to

$$p(\underline{x}_k|\underline{Z}_k) = \mathcal{N}(\underline{x}_k - \mu_k, \Sigma_k) \tag{11}$$

and

$$p(\underline{x}_k|\underline{Z}_{k-1}) = \mathcal{N}(\underline{x}_{k|k-1} - \mu_{k|k-1}, \Sigma_{k|k-1}) \ . \tag{12}$$

As the system model is linear, the prediction step can be performed analytically according to

$$\mu_{k|k-1} = \mathbf{A} \cdot \mu_{k-1} \ , \tag{13}$$

$$\Sigma_{k|k-1} = \mathbf{A} \cdot \Sigma_{k-1} \cdot \mathbf{A}^T + \mathbf{C}_v \ . \tag{14}$$

The measurement equation (6) is highly nonlinear, e.g., it is symmetric in the object states and it contains non-additive measurement noise. In order to perform the measurement update step, we proffer the Gaussian particle filter [20], which allows for working with the mean and covariance matrix for the state as in (11) and (12).

With the prediction as a proposal density [20], we obtain the following algorithm for the measurement update:

1) Draw N_p samples $\{\mathrm{x}^{(i)}\}_{i=1}^{N_p}$ from the prediction $\mathcal{N}(\underline{x}_{k|k-1} - \mu_{k|k-1}, \Sigma_{k|k-1})$.
2) Calculate a particle approximation of the posterior consisting of the particle locations $\{\mathrm{x}^{(i)}\}_{i=1}^{N_p}$ and weights

$$w_i = \frac{p(\underline{z}_k \,|\, \mathrm{x}^{(i)})}{\sum_{i=1}^{N_p} p(\underline{z}_k \,|\, \mathrm{x}^{(i)})} \ . \tag{15}$$

3) Calculate the sample mean and covariance of $\{\mathrm{x}^{(i)}\}_{i=1}^{N_p}$

$$\mu_k = \sum_{i=1}^{N_p} w_i \cdot \mathrm{x}^{(i)} \ , \tag{16}$$

$$\Sigma_k = \sum_{i=1}^{N_p} w_i \cdot (\mathrm{x}^{(i)} - \mu_k) \cdot (\mathrm{x}^{(i)} - \mu_k)^T \tag{17}$$

The Gaussian particle filter in its original formulation is tailored for optimizing the posterior mean of the state, i.e., it minimizes the mean squared error

$$\underline{\hat{x}}_k^{\mathrm{MMSE}} := \arg\min_{\underline{\hat{x}}_k} \int ||\underline{\hat{x}}_k - \underline{x}_k||^2 \ p(\underline{x}_k \,|\, \underline{Z}_k) \ d\underline{x}_k \ . \tag{18}$$

But MMSE estimates suffer markedly from track coalescence where there is a symmetric likelihood, as might happen due to exchangeability of objects [3]. In fact, the received signal $\underline{z}_k^m$ in (5) is composed of sums representing the individual signals, i.e., $\underline{x}_l$ and $\underline{s}_l$. Hence, the ship states can be permuted without changing the measurement $\underline{z}_k^m$. For example, let there be two ships with

- $\theta_1 = 0.1$ and $\underline{s}_1 = 2$ for ship 1, and
- $\theta_2 = 0.3$ and $\underline{s}_2 = 1$ for ship 2.

If we switch the labels “ship 1” and “ship 2”, the received signal $\underline{z}_k^m$ does not change, i.e.,

- $\theta_2 = 0.1$ and $\underline{s}_2 = 2$ for ship 1, and
- $\theta_1 = 0.3$ and $\underline{s}_1 = 1$ for ship 2.

This means that the received signal does not contain labeling information about the ships, i.e., it is unknown which signal comes from which ship. Hence, the likelihood function (7) for DOA estimation is symmetric in the ship states.

As the prior density loses its influence on the posterior density over time, the posterior progressively becomes more symmetric (for closely-spaced ships). Reasonably, the mean of a multi-object probability density that is symmetric in the object states *always* coalesces objects.

A detailed discussion and illustration of this phenomenon can be found in [3], for example. In the Gaussian particle filter, the described problems of the MMSE estimate can result in a mean (16) that coalesces closely-spaced ships, which is highly undesired.

IV. Set Gaussian Particle Filter (Set-GPF)

This section shows how the Gaussian particle filter presented in the previous section can be tailored to prevent track coalescence with the help of MMOSPA estimation techniques.

A systematic solution to the problems of MMSE estimation described previously is to ignore the labels of the objects. For this purpose, the basic idea is to replace the squared error in the MMSE definition with a permutation invariant criterion called *Optimal Sub-Pattern Assignment (OSPA)* [27] distance. The OSPA distance is considered as the standard metric for performance evaluation of multi-object trackers. For two vectors $\underline{x} = [(\underline{x}^1)^T, \ldots, (\underline{x}^{N_t})^T]^T$ and $\underline{y} = [(\underline{y}^1)^T, \ldots, (\underline{y}^{N_t})^T]^T$, which consist of N_t state vectors, the OSPA distance is defined as

$$\text{OSPA}(\underline{x}, \underline{y})^2 := \frac{1}{N_t} \min_{\pi \in \Pi_{N_t}} ||\underline{x} - P_\pi(\underline{y})||^2 \ , \tag{19}$$

where Π_{N_t} denotes all permutations of the set $\{1, \ldots, N_t\}$ and $P_\pi(\underline{x}) := [(\underline{x}^{\pi(1)})^T, \ldots, (\underline{x}^{\pi(N_t)})^T]^T$ permutes the single object states in $\underline{x}$ according to π. The OSPA distance is a metric on sets. For two sets with equal cardinality as in (19), the OSPA distance coincides with the Wasserstein distance [32].

Based upon (19), the Minimum Mean Optimal Sub-Pattern Assignment (MMOSPA) can be defined [18] in analogy to the MMSE estimate, i.e.,

$$\underline{\hat{x}}_k^{\text{MMOSPA}} := \arg\min_{\underline{\hat{x}}_k} \int \text{OSPA}(\underline{x}_k, \underline{\hat{x}}_k)^2 \ p(\underline{x}_k | Z_k) \ d\underline{x} \ . \tag{20}$$

There are always $N_t!$ equivalent MMOSPA estimates because all permutations of a specific $\underline{\hat{x}}_k^{\text{MMOSPA}}$ also minimize (20).

Due to permutation invariance in the definition of the OSPA distance, the MMOSPA estimate does not coalesce even for closely-spaced objects, see also the discussion in [3].

There are various efficient approximations available [12], [14], [18] for calculating MMOSPA estimates. In case of a particle representation exact efficient algorithms are available for two objects and one-dimensional objects [2], [5].

In order to tailor the Gaussian particle filter to perform well with respect to the OSPA metric, we propose the following modification of the measurement update step:

- Replace the sample mean of the particles $\{\text{x}^{(i)}\}_{i=1}^{N_p}$ in (16) with the MMOSPA estimate of the particles, and
- replace the sample covariance matrix of the particles $\{\text{x}^{(i)}\}_{i=1}^{N_p}$ in (17) with the unordered joint covariance [10] of the particles,

which yields

$$\begin{aligned} \mu_k &= \arg\min_{\underline{\hat{x}}_k} \sum_{i=1}^{N_p} w_i \cdot \text{OSPA}(\text{x}^{(i)}, \underline{\hat{x}}_k)^2 \ , & (21) \\ \Sigma_k &= \sum_{i=1}^{N_p} w_i \cdot \min_{\pi \in \Pi_{N_t}} (P_\pi(\text{x}^{(i)}) - \mu_k) \cdot \\ &\quad (P_\pi(\text{x}^{(i)}) - \mu_k)^T \ . & (22) \end{aligned}$$

instead of (16) and (17).

The above modifications ensure that the Gaussian approximation of the symmetric posterior follows a single "mode". But of course, the labeling information of the ships gets lost.

There are efficient algorithms available for calculating the MMOSPA estimate for empirical distributions, i.e., for performing the optimization (21). For example, [18] proposed an iterative approximate algorithm, and [2], [5] derived exact algorithms. Having calculated the MMOSPA estimate (21), it is straightforward to determine the unordered joint covariance (22). Note that the problem of calculating (21) is equivalent to the problem of calculating a Wasserstein Barycenter [1], [6], [8], [15] as described in [4].

V. Experimental Results

In order to evaluate the Set-GPF introduced in the previous section, we consider two scenarios from the SWAP experiments where two ships cross each others' paths in DOA space. Specifically, on September 7, 2007, between 16:00 pm and 17:20 pm the tracks of two ships "Island Adventure" and "Seward Johnson" cross twice in DOA space. The ship "Seward Johnson" is a research vessel that is part of the SWAP experiments. It is equipped with an acoustic source for evaluating the characteristic of the shallow water environment. We do not have any information about the ship "Island Adventure" available. Its signals are coincidentally detected by the sonar array. The AIS data for the ships serves as a ground truth. In both scenarios, we use 40 hydrophones from the sonar array. In order emulate different conditions, the scenarios involve different parameters for the signal processing.

A. Scenario 1

The first scenario deals with the first crossing of the two ships between 16:00 pm and 16:40 pm. The specific parameters are as follows:

- Passband: $200\,\text{Hz}$-$210\,\text{Hz}$
- Carrier frequency: $205\,\text{Hz}$
- Time interval: $5\,\text{s}$
- Total number of time steps: 280
- System noise: $q_0 = 0.000001$
- Measurement noise: $\mathbf{C}_v = 0.001$ and $\mathbf{C}_s = 0.001$
- Number of particles: 5000

The ground truth and the estimation results are depicted in Fig. 2. First, note that the Set-GPF apparently does not detect the tracks' crossing. This may seem unfortunate, but is actually a rather natural by-product of its ability to maintain track on even closely-spaced objects. That is: since identity (labeling) has no meaning to MMOSPA (nor, hence, to the Set-GPF) the event of a cross, as opposed to a "bounce", is a similarly alien concept to it. On the other hand, the results clearly show that the standard GPF tends to coalesce the tracks; and the Set-GPF does not. That is, the Set-GPF has done what it has been designed to do.

B. Scenario 2

The second scenario consider the time span from 16:30 pm and 17:20 pm in which the ships cross for the second time. The specific parameters are as follows:

- Passband: $410\,\text{Hz}$-$415\,\text{Hz}$
- Carrier frequency: $412.5\,\text{Hz}$
- Time interval: $10\,\text{s}$
- Total number of time steps: 300
- System noise: $q_0 = 0.000001$
- Measurement noise: $\mathbf{C}_v = 0.001$ and $\mathbf{C}_s = 0.001$
- Number of particles: 5000

The ground truth and the estimation results are plotted in Fig. 3. It appears that the passband from $410\,\mathrm{Hz}$ to $415\,\mathrm{Hz}$ gives a more precise BTR of the tracks than the passband in Scenario 1. In contrast to the first scenario, this scenario considers a longer time frame, but the time steps are also longer. The results are similar to the first scenario: The GPF coalesces the target but the Set-GPF is able to follow the tracks accurately. The Set-GPF does not exhibit a "crossing" behavior; but that is not expected.

VI. Conclusions

Directions-of-arrival estimation of multiple signals impinging on a sensor array is a fundamental signal processing problem with many applications. A main challenge is to resolve different directions-of-arrivals from closely-spaced objects. For this purpose, we proffer the concept of minimum mean OSPA estimation, which was recently developed for optimizing multi-object tracking algorithms with respect to a set metric. MMOSPA estimation techniques have been applied to DOA estimation before, see [3], [10], [11]. The contribution of this work is to demonstrate the benefits of MMOSPA for DOA tracking by means of real data from a large sonar array that is part of the SWAP project. In order to deal with the nonlinearity of the DOA estimation problem, we develop a set-variant of the Gaussian particle filter (called Set-GPF), which is in the line of the Set-JPDAF [29] and Set-MHT [13]. We present two scenarios from the SWAP data set in which the Set-GPF is able to track two crossing objects, while the traditional Gaussian particle filter fails by coalescing the tracks. As a simplifying assumption, we assumed that the number of objects in the surveillance region is known in advance. In future work, we plan to drop this assumption and develop an integrated MMOSPA approach for simultaneous object tracking and number estimation. Also, it is possible to reintroduce the track labels such as in [16].

Acknowkledgments

This research was supported by the Office of Naval Research under contract N000014-13-1-0231. We would like to thank Dr. Lisa Zurk of Portland State University and Dr. John Tague from the Office of Naval Research for making available the SWAP data set and its associated source code for the signal processing and visualization.

References

[1] M. Agueh and G. Carlier, "Barycenters in the Wasserstein Space," *SIAM Journal on Mathematical Analysis*, vol. 43, no. 2, pp. 904–924, 2011.

[2] M. Baum, P. Willett, and U. D. Hanebeck, "Calculating Some Exact MMOSPA Estimates for Particle Distributions," in *Proceedings of the 15th International Conference on Information Fusion (Fusion 2012)*, Singapore, Jul. 2012.

[3] ——, "MMOSPA-based Direction-of-Arrival Estimation for Planar Antenna Arrays," in *Proceedings of the Eighth IEEE Sensor Array and Multichannel Signal Processing Workshop (SAM 2014)*, A Coruña, Spain, Jun. 2014.

[4] ——, "On Wasserstein Barycenters and MMOSPA Estimates," *IEEE Signal Processing Letters*, vol. 22, no. 10, pp. 1511–1515, Oct. 2015.

[5] ——, "Polynomial-Time Algorithms for the Exact MMOSPA Estimate of a Multi-Object Probability Density Represented by Particles," *IEEE Transactions on Signal Processing*, vol. 63, no. 10, pp. 2476–2484, May 2015.

[6] J. Bigot and T. Klein, "Consistent Estimation of a Population Barycenter in the Wasserstein Space," *ArXiv e-prints*, Dec. 2012.

[7] R. L. Campbell and L. M. Zurk, "Effect on Surface Ship Interference on Adaptive Beamforming for the Shallow Water Array Performance (SWAP) Project," *The Journal of the Acoustical Society of America*, vol. 122, no. 5, pp. 3022–3022, 2007.

[8] G. Carlier, A. Oberman, and E. Oudet, "Numerical Methods for Matching for Teams and Wasserstein Barycenters," Tech. Rep., May 2014.

[9] D. F. Crouse, P. Willett, and Y. Bar-Shalom, "Developing a Real-Time Track Display That Operators Do Not Hate," *IEEE Transactions on Signal Processing*, vol. 59, no. 7, pp. 3441–3447, Jul. 2011.

[10] D. F. Crouse, P. Willett, Y. Bar-Shalom, and L. Svensson, "Aspects of MMOSPA Estimation," in *Proceedings of the 50th IEEE Conference on Decision and Control and European Control Conference, Orlando, FL*, Dec. 2011.

[11] D. F. Crouse, P. Willett, L. Svensson, and Y. Bar-Shalom, "Comparison of Compressed Sensing, ML, and MMOSPA Estimation for Radar Superresolution," in *Proc. 45th Asilomar Conference on Signals, Systems and Computers*, 2011.

[12] D. F. Crouse, "Advances in Displaying Uncertain Estimates of Multiple Targets," in *SPIE – Signal Processing, Sensor Fusion, and Target Recognition XXII*, vol. 8745, 2013, pp. 874 504–874 504–31.

[13] D. F. Crouse, P. Willett, L. Svensson, D. Svensson, and M. Guerriero, "The Set MHT," in *Proceedings of the 14th International Conference on Information Fusion (Fusion 2011)*, Jul. 2011.

[14] D. F. Crouse, P. Willett, M. Guerriero, and L. Svensson, "An Approximate Minimum MOSPA Estimator," in *IEEE International Conference on Acoustics, Speech and Signal Processing (ICASSP)*, May 2011, pp. 3644 –3647.

[15] M. Cuturi and A. Doucet, "Fast Computation of Wasserstein Barycenters," in *Proceedings of the 31st International Conference on Machine Learning (ICML-14)*, Oct. 2014.

[16] R. Georgescu, P. Willett, L. Svensson, and M. Morelande, "Two Linear Complexity Particle Filters Capable of Maintaining Target Label Probabilities for Targets in Close Proximity," in *15th International Conference on Information Fusion (FUSION)*, 2012, pp. 2370–2377.

[17] L. Godara, "Application of Antenna Arrays to Mobile Communications. II. Beam-forming and Direction-of-arrival Considerations," *Proceedings of the IEEE*, vol. 85, no. 8, pp. 1195–1245, Aug 1997.

[18] M. Guerriero, L. Svensson, D. Svensson, and P. Willett, "Shooting Two Birds with Two Bullets: How to Find Minimum Mean OSPA Estimates," *Proceedings of the 13th International Conference on Information Fusion (Fusion 2010)*, 2010.

[19] K. D. Heaney and J. J. Murray, "Measurements of Three-Dimensional Propagation in a Continental Shelf Environment," *The Journal of the Acoustical Society of America*, vol. 125, no. 3, pp. 1394–1402, 2009.

[20] J. Kotecha and P. Djuric, "Gaussian Particle Filtering," *IEEE Transactions on Signal Processing*, vol. 51, no. 10, pp. 2592 – 2601, Oct. 2003.

[21] C. Kreucher and B. Shapo, "A Fuse-Before-Track Approach to Target State Estimation using Passive Acoustic Sensors," in *Proceedings of the 14th International Conference on Information Fusion (FUSION)*, Jul. 2011.

[22] R. Mahler, "Statistics 101 for Multisensor, Multitarget Data Fusion," *IEEE Aerospace and Electronic Systems Magazine*, Vol. 19, No. 1, Part 2, pp. 53-64, January 2004.

[23] R.P.S. Mahler, "Statistical Multisource-Multitarget Information Fusion," *Artech House*, 2007.

[24] ——, "Array Processing for Radar: Achievements and Challenges," *International Journal of Antennas and Propagation*, vol. 2013, p. 21, 2013.

[25] B. Ottersten, M. Viberg, P. Stoica, and A. Nehorai, "Exact and Large Sample Maximum Likelihood Techniques for Parameter Estimation and Detection in Array Processing," in *Radar Array Processing*, ser. Springer Series in Information Sciences, S. Haykin, J. Litva, and T. Shepherd, Eds. Springer Berlin Heidelberg, 1993, vol. 25.

[26] K. Scarbrough, S. Mitchell and J. Hovenga,"Shallow Water Array Performance (SWAP): Array Element Localization and Performance

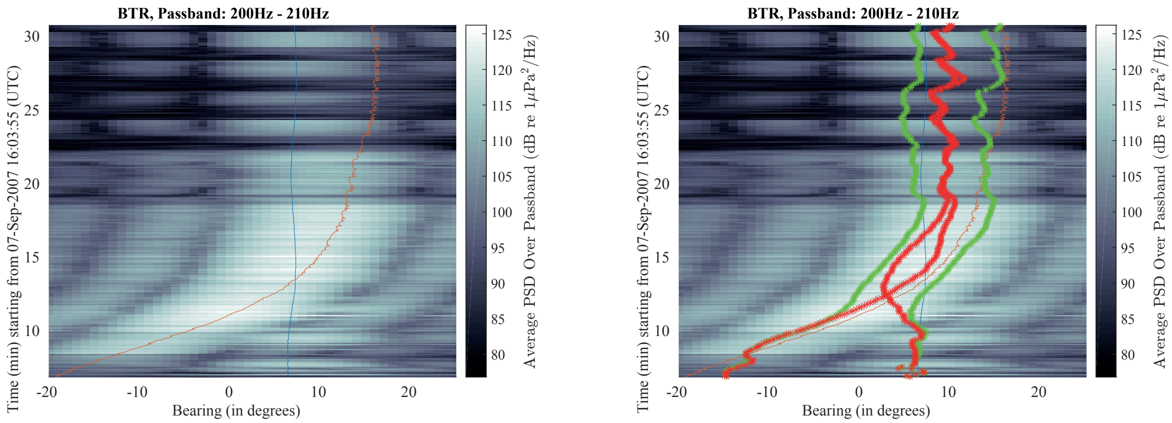

(a) BTR and AIS tracks of two crossing ships.

(b) Tracking results of the GPF (red) and Set-GPF (green).

Fig. 2: Ground truth and tracking results for Scenario 1.

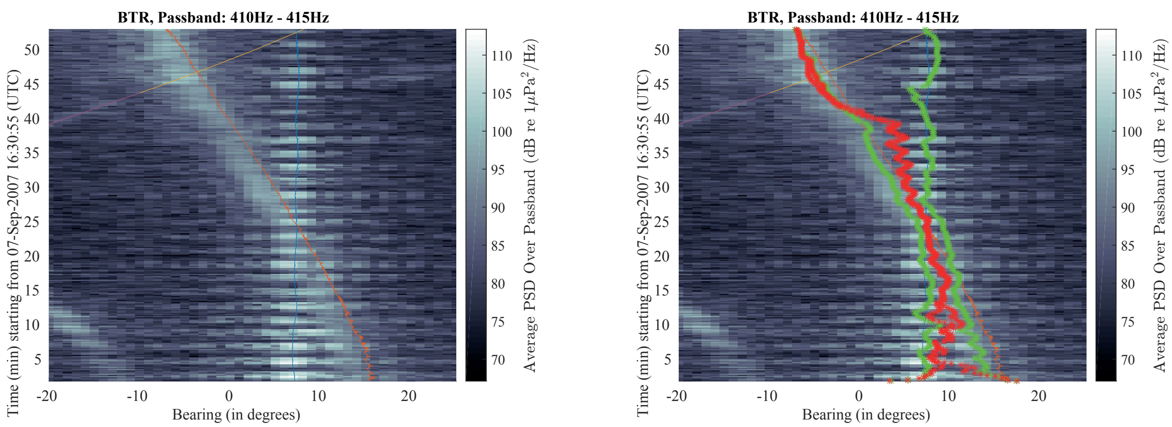

(a) BTR and AIS tracks of two crossing ships.

(b) Tracking results of the GPF (red) and Set-GPF (green).

Fig. 3: Ground truth and tracking results for Scenario 2.

Characterization," University of Texas at Austin, Applied Research Laboratories, Tech. Rep., 2007.

[27] D. Schuhmacher, B.-T. Vo, and B.-N. Vo, "A Consistent Metric for Performance Evaluation of Multi-Object Filters," *IEEE Transactions on Signal Processing*, vol. 56, no. 8, pp. 3447 –3457, 2008.

[28] P. Stoica and K. Sharman, "Maximum Likelihood Methods for Direction-of-Arrival Estimation," *IEEE Transactions on Acoustics, Speech and Signal Processing*, vol. 38, no. 7, pp. 1132–1143, Jul 1990.

[29] L. Svensson, D. Svensson, M. Guerriero, and P. Willett, "Set JPDA Filter for Multi-Target Tracking," *IEEE Transactions on Signal Processing*, vol. 59, no. 10, pp. 4677-4691, 2011.

[30] J.-M. Valin, F. Michaud, and J. Rouat, "Robust Localization and Tracking of Simultaneous Moving Sound Sources Using Beamforming and Particle Filtering," *Robotics and Autonomous Systems*, vol. 55, no. 3, pp. 216 – 228, 2007. [Online].

[31] H. L. Van Trees, *Optimum Array Processing*. John Wiley & Sons, Inc., 2002.

[32] C. Villani, *Optimal Transport*. Springer Verlag, 2009.

[33] D. B. Ward, E. Lehmann, and R. Williamson, "Particle Filtering Algorithms for Tracking an Acoustic Source in a Reverberant Environment," *IEEE Transactions on Speech and Audio Processing*, vol. 11, no. 6, pp. 826–836, Nov 2003.

[34] X. Zhong, A. Premkumar, and W. Wang, "Direction of Arrival Tracking of an Underwater Acoustic Source Using Particle Filtering: Real Data Experiments," in *IEEE TENCON Spring Conference*, April 2013, pp. 420–424.